2011 American Control Conference
on O'Farrell Street, San Francisco, CA, USA
June 29 - July 01, 2011

Reduced-Order Modal-Domain Structural Control for Seismic Vibration Control Over Wireless Sensor Networks

R. Andrew Swartz, *Associate Member, ASCE*

Abstract—**Semi-active control devices are promising technologies to provide economical and reliable protection for the safety of civil infrastructure assets as well as preserving the comfort of their occupants due to their low costs and power requirements. However, these devices can be limited in their capacity to provide large control forces necessitating installations in large numbers, creating additional expense and vulnerabilities to the system in the form of extensive lengths of signal cables. Wireless sensor networks are gaining popularity as a means of collecting, coordinating, and processing data from spatially distributed locations in civil structures. Their inherent computational abilities can also be harnessed to command networks of structural control actuators, however significant issues exist with regard to communication delays and computational power that must be addressed. This study demonstrates the successful application of a modal-domain state-space control algorithm for use in wireless structural control of a six-story shear building with magneto-rheological actuators. Control laws and state estimators are derived in modal coordinates for models of increasing size. Increasing the complexity of the underlying model yields a more optimal control law; however due to the limitations of the wireless actuator nodes in computational power, this increase in complexity comes at the expense of significantly increased latency which degrades performance. The trade-off between speed and model order is explored in terms of control performance. Both simulation and experimental results are presented.**

I. Introduction

CIVIL engineering structures are continually subjected to deleterious effects of the environment in which they are constructed (with wind and seismic loadings representing two of the most significant stochastic hazards). Civil structural design has evolved to protect building occupants during extreme stochastic events (*e.g.*, large earthquakes) occasionally at the cost of the structure itself. Ductile design of buildings ensures energy dissipation during large earthquakes through yielding of lateral load support members. The resulting damage may require significant repair or even replacement of the structure. For high-value structures, including critical planning facilities and emergency response centers, evacuation is often not acceptable. In such cases, it may be preferable to dissipate seismically induced energy through use of a structural control system [1-3]. Control devices may be designed to reject unwanted disturbances created by wind or seismic forces offering both protection for the structure and enhanced comfort for its occupants. One approach would be the use of passive devices (*e.g.*, tuned-mass or tuned-liquid dampers) that could reduce the effects of lateral excitations near the fundamental resonant frequency of the structure. Such devices are limited in the amount of control authority they can provide. Active control technologies, (*e.g.*, active mass dampers) can produce very good control effects, but are typically very costly to install and rely on large amounts of external power to operate. In recent years, semi-active control devices (*e.g.*, variable-orifice dampers, variable-stiffness braces, magneto-rheological or electro-rheological dampers, *etc*.) have become available as an attractive combination of the two previous approaches [4]. These devices impart control forces indirectly by making strategic, real-time changes in structural parameters. As such, large numbers (potentially in the hundreds) of these devices are necessary to achieve satisfactory control performance. As with the installation of sensors in civil structures, the installation of dedicated signal lines in buildings or bridges introduces a significant new cost (a few thousand dollars per channel [5]) reducing their attractiveness. One solution is to forego data connections between devices [6] sacrificing the advantages that can be gained through coordination. However, another solution is the introduction of wireless sensing and actuation nodes that can collect response data, compute control forces, and issue commands to collocated actuators in real time.

Wireless control nodes are not a perfect replacement for traditional tethered systems. Limitations in computational power, memory, communication bandwidth, and energy (in battery powered networks) present significant challenges. Wang, *et al*. [7] used wireless actuation networks to compute and command magneto-rheological dampers to reject seismic excitations in a three-story building. By limiting communications between sensors, Wang *et al*. [8, 9] were able to increase the speed of the network by decreasing latency due to wireless data transmission and improve control performance by varying the communication topology for the same three-story structure as well as for a six-story structure. Utilizing a faster wireless radio, Swartz and Lynch [10] were able to decrease latency due to communication for control of the six-story structure and improved communication channel performance by limiting data transferred between units. Reducing communication between wireless nodes can improve performance by

Manuscript received September 27, 2010.

R. A. Swartz is an Assistant Professor with appointments in the Department of Civil and Environmental Engineering and the Department of Electrical and Computer Engineering at Michigan Technological University, Houghton, MI 49931 (phone: 906-487-2439; fax: 906-487-2943; e-mail: raswartz@ mtu.edu).

decreasing latency, but the practice of not sharing data between units increases the computational burden placed on the wireless computers. Embedded estimators must compute the unknown state data and the number of floating-point computations required to do so increases dramatically with the number of degrees of freedom (DOF) in the structure. In resource-constrained wireless networks, these floating-point computations can represent a significant source of latency and negatively impact control performance.

This study investigates the use of reduced-order models for control of civil structures over wireless networks. By sacrificing model fidelity, it will be possible to decrease latency in the controller. Modal-domain condensation of the model is employed to reduce the size of the state-space model used by the controller and associated state estimator. As the size of the model decreases, the size of the time step required by the wireless actuator units to sense, compute, and actuate also decreases. The tradeoff between model size and time step length is investigated both in simulation and experimentally.

In the next section, the theoretical underpinnings for the algorithm used in this study are presented. The following section introduces the wireless sensor and actuator network used in this study and also includes a description of the methods and setup for the simulation and experimental studies. Next, results from the two phases of the study are presented followed by discussion and conclusions.

II. Theory

The multiple-input multiple-output (MIMO) control approach used for this study is based on a state-space representation of equation of motion for a six-story lumped-mass shear structure:

$$\mathbf{M}\ddot{\mathbf{x}}(t)+\mathbf{C_d}\dot{\mathbf{x}}(t)+\mathbf{K}\mathbf{x}(t)=-\mathbf{M}\ell\ddot{x}_g(t)+\mathbf{L}\mathbf{u}(t) \tag{1}$$

where $\boldsymbol{x}$ is the vector of lateral floor displacements, $\boldsymbol{M}$, $\boldsymbol{C_d}$, and $\boldsymbol{K}$ are the structural mass, damping, and stiffness matrices respectively, $\boldsymbol{u}$ is the vector of control forces, $\boldsymbol{L}$ gives the configuration of the actuators, and ℓ is a vector of ones. The state space representation of Eqn. (1) is:

$$\begin{aligned}\dot{\mathbf{z}}(t)&=\mathbf{A}\mathbf{z}(t)+\mathbf{B}\mathbf{u}(t)+\mathbf{E}\ddot{x}_g(t)\\ \mathbf{y}(t)&=\mathbf{C}\mathbf{z}(t)+\mathbf{D}\mathbf{u}(t)+\mathbf{F}\ddot{x}_g(t)\end{aligned} \tag{2}$$

$$\mathbf{A}=\begin{bmatrix}\mathbf{0} & \mathbf{I}\\ -\mathbf{M}^{-1}\mathbf{K} & -\mathbf{M}^{-1}\mathbf{C_d}\end{bmatrix}\qquad \mathbf{B}=\begin{bmatrix}\mathbf{0}\\ \mathbf{M}^{-1}\mathbf{L}\end{bmatrix}\qquad \mathbf{E}=\begin{bmatrix}\mathbf{0}\\ -\ell\end{bmatrix} \tag{3}$$

and $\boldsymbol{C}$, $\boldsymbol{D}$, and $\boldsymbol{F}$ are dependent on the sensor output. For inter-story drift feedback:

$$\boldsymbol{C}=\begin{bmatrix}[\mathbf{0}] & \begin{bmatrix}1 & & 0\\ -1 & \ddots & \\ 0 & -1 & 1\end{bmatrix}\end{bmatrix}\qquad \mathbf{D}=[\mathbf{0}]\qquad \mathbf{F}=[\mathbf{0}] \tag{4}$$

For acceleration feedback:

$$\boldsymbol{C}=[-\boldsymbol{M}^{-1}\boldsymbol{K}\quad -\boldsymbol{M}^{-1}\boldsymbol{C}_d]\qquad \boldsymbol{D}=[-\boldsymbol{M}^{-1}\boldsymbol{L}]\qquad \boldsymbol{E}=[-\ell] \tag{5}$$

An optimal control law can be derived for this system based on LQR control that minimizes the cost function, J:

$$J(\mathbf{u})=\sum_{k=1}^{\infty}\left(\mathbf{z}^T(k)\mathbf{Q}_1\mathbf{z}(k)+\mathbf{u}^T(k)\mathbf{Q}_2\mathbf{u}(k)\right) \tag{6}$$

where $\boldsymbol{Q_1}$ and $\boldsymbol{Q_2}$ are weighting matrices that balance control effort expended against control performance [11]. The optimal control force is given by:

$$\boldsymbol{u}(t)=-\boldsymbol{G}\boldsymbol{z}(t)=-[[\boldsymbol{Q_2}+\boldsymbol{B}^{\mathrm{T}}\boldsymbol{P}\boldsymbol{B}]^{-1}\boldsymbol{B}^{\mathrm{T}}\boldsymbol{P}\boldsymbol{A}]\boldsymbol{z}(t) \tag{7}$$

where $\boldsymbol{P}$ is the solution to the algebraic Riccati equation. To implement the controller on a digital computer, conversion to a discrete time model is necessary. Using a zero-order hold approximation, the state-space representation becomes:

$$\mathbf{z}(k+1)=\mathbf{\Phi}\mathbf{z}(k)+\mathbf{\Gamma}\mathbf{u}(k)+\mathbf{\Lambda}\ddot{x}_g(k) \tag{8}$$

$$\mathbf{\Phi}=e^{\mathbf{A}T_S}\qquad \mathbf{\Gamma}=\left(\int_0^{T_S}e^{\mathbf{A}\tau}d\tau\right)\mathbf{B}\qquad \mathbf{\Lambda}=\left(\int_0^{T_S}e^{\mathbf{A}\tau}d\tau\right)\mathbf{E} \tag{9}$$

where T_s is the time step of the controller [12]. Because direct measurement of the entire state vector is impractical for this application, an optimal Kalman-based state estimator is employed that seeks to minimize the covariance:

$$\boldsymbol{P_e}=\lim_{t\to\infty}[(\boldsymbol{z}-\hat{\boldsymbol{z}})(\boldsymbol{z}-\hat{\boldsymbol{z}})^{\mathrm{T}}] \tag{10}$$

where $\hat{\boldsymbol{z}}$ is the state estimate [12]. By treating the estimation error as a disturbance to be rejected, an optimal control gain $\boldsymbol{L}$ is derived that estimates the full state vector according to:

$$\hat{\boldsymbol{z}}(k+1)=\bar{\boldsymbol{z}}(k+1)+\boldsymbol{L}((\boldsymbol{y}(k)-\boldsymbol{C}\hat{\boldsymbol{z}}(k)) \tag{11}$$

where:

$$\bar{\boldsymbol{z}}(k+1)=\mathbf{\Phi}\hat{\boldsymbol{z}}(k)+\mathbf{\Gamma}\boldsymbol{u}(k) \tag{12}$$

Combining terms can gain some computational efficiency:

$$\hat{\boldsymbol{z}}(k+1)=\boldsymbol{A_{est}}\hat{\boldsymbol{z}}(k)+\boldsymbol{B_{est}}\boldsymbol{y}(k) \tag{13}$$

$$\boldsymbol{A_{est}}=\mathbf{\Phi}-\mathbf{\Gamma}\boldsymbol{G}-\boldsymbol{L}\boldsymbol{C}\qquad \boldsymbol{B_{est}}=\boldsymbol{L} \tag{14}$$

The effectiveness of the controller (in terms of rejecting transient disturbances) is dependent both the size of the time step used in the zero-order hold approximation, as well as the accuracy of the estimator. The size of the time step is dependent on the speed of the digital computer responsible for computing control forces; in wireless control nodes, this delay can become significant with just a few DOFs. If the size of the underlying model can be reduced, the size of the time step may be reduced as well. In this study, modal condensation is used to reduce the model size by eliminating higher order modes (those that have the highest frequency) that are less dominant in the response of the structure.

To derive the reduced-order model, the system must first be converted into modal coordinates. The i^{th} column of the conversion matrix, $\boldsymbol{\Psi}$, used for this conversion is the i^{th} mode shape, $\boldsymbol{\psi}_i$ (length normalized to 1), derived from the eigenvectors of:

$$\boldsymbol{\Psi}=[\boldsymbol{\psi}_1\quad\cdots\quad\boldsymbol{\psi}_n] \tag{15}$$

$$\boldsymbol{\psi}_i=\mathrm{eigenvectors}(\boldsymbol{M}^{-1}\boldsymbol{K}) \tag{16}$$

where n is the number of floors in the structure. A change of basis matrix, $\boldsymbol{T_0}$, is constructed from the relationship:

$$\boldsymbol{T_0} = \begin{bmatrix} \boldsymbol{\Psi} & \boldsymbol{0} \\ \boldsymbol{0} & \boldsymbol{\Psi} \end{bmatrix} \quad (17)$$

and the modal-domain representation of the system is:

$$\begin{matrix} \boldsymbol{A_0} = \boldsymbol{T_0^{-1}AT_0} & \boldsymbol{B_0} = \boldsymbol{T_0^{-1}B} & \boldsymbol{E_0} = \boldsymbol{T_0^{-1}E} \\ \boldsymbol{C_0} = \boldsymbol{CT_0} & \boldsymbol{D_0} = \boldsymbol{D} & \boldsymbol{F_0} = \boldsymbol{F} \end{matrix} \quad (18)$$

The reduced representation of the system is derived by removing the rows and columns of the state-space matrices associated with the higher order modes. The accuracy of the resulting estimator is dependent upon the participation of these high-order modes in the response of the structure (low for many seismically excited civil structures). With the reduced, continuous-time representation computed, derivation of the optimal LQR control law, the discrete-time model, and the Kalman estimator may then proceed as described above. The size of the control and estimation matrices ($\boldsymbol{G_r}$, $\boldsymbol{A_{est\_r}}$, and $\boldsymbol{B_{est\_r}}$) will then be dependent on the number of sensors, p, the number of controllers, q, and the number of states retained, m:

$$\boldsymbol{G_r} \in \mathbb{R}^{qxm} \qquad \boldsymbol{A_{est\_r}} \in \mathbb{R}^{mxm} \qquad \boldsymbol{B_{est\_r}} \in \mathbb{R}^{mxp} \quad (19)$$

The ultimate time step achievable for a given model size, m, is a function of the wireless computing platform used. The platform used in this study is detailed in the following section.

III. Methods

A. *Narada Wireless Sensing and Actuation Platform*

A wireless sensor platform is used to collect data in situations where installation of dedicated data cables is excessively expensive or onerous. To accomplish its task a sensor interface is required to convert (usually analog) transducer signals into digital numbers, a wireless radio is required to receive commands and send results to users, and a computational core is required to coordinate sensing, data storage, and communication tasks within the sensor as well as perform embedded data interrogation (if required). In wireless control networks, an actuation interface is also required to send analog command signals to collocated actuators. In battery powered wireless networks, all of these components must be as power efficient as possible to keep maintenance costs (due to battery replacement) from eroding the cost savings realized by use of wireless sensors. This power limitation will limit computational speed of the microcontroller. This limitation in wireless control networks has a direct effect on the controller speed.

In this study, the *Narada* wireless sensing and actuation platform (Fig. 1) is used for the experimental study and provides the performance specifications used in the computational study. The *Narada* platform was developed by Swartz, *et al.* [13] for sensing and actuation applications in civil structures. For a sensing interface, it has a Texas Instruments ADS8341, 4-channel, 16-bit analog-to-digital

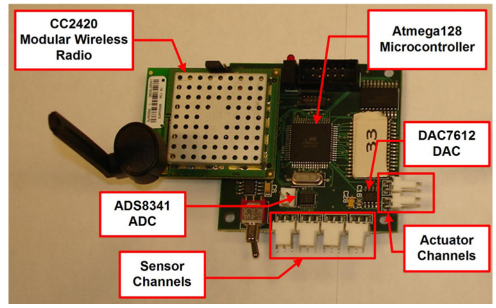

Fig. 1. *Narada* wireless sensing and actuation node.

converter (ADC). The wireless communication interface is the Chipcon CC2420, an IEEE802.15.4 compliant wireless transceiver designed to form and participate in adaptive *ad-hoc* sensor networks. The actuation interface is a Texas Instruments DAC7612, 2-channel, 12-bit digital-to-analog converter (DAC). The key aspect of the *Narada* unit with relation to this study is the computational core, the Atmel Atmega128 microcontroller. The Atmega128 is an 8-bit AVR microcontroller with 128 kB of flash memory, 4 kB of on-board SRAM, and 4 kB of EEPROM. On *Narada*, it operates at a clock speed of 8 MHz and is augmented with an additional 128 kB of external SRAM for data storage. The AVR core executes each assembly instruction in a single clock cycle, but floating point computations required in state-space estimation and feedback control require multiple instructions (and therefore, multiple clock cycles) per mathematical operation. This computational time becomes significant as the model size grows large.

B. *Computational and Simulation Study*

Validation of the approach is performed both within the simulation environment and experimentally using a scale, six-story steel laboratory specimen as the test structure (Fig. 2). The structure has a 1.0m x 1.5m footprint and is 1.0 m high from floor to floor (6 m high in total). The mass of each floor is taken as approximately 640 kg, the structure has story stiffness values of approximately 2.4×10^6 N/m, and damping is assumed to be 1.25% Rayleigh damping [14]. The simulation models the effects on the structure of dynamic unidirectional lateral ground motion based on the El Centro 1940 NS (USGS Station 117) ground record that has been scaled to a peak acceleration of 1.0 m/s^2 (100 gals). Modal-space control requires the conversion of the model from standard coordinates (Fig. 3, top) to modal coordinates (Fig. 3, bottom), found from Eqn. 16. Simulations are performed in the Matlab environment using Newmark integration [14] to update the equation of motion.

The LQR control formulation is based on penalizing inter-story drift in the structure. Inter-story drift is linked to damage of structural and non-structural components. The LQR formulation (in modal coordinates) used in both the simulation and experimental portions of this study is:

$$\boldsymbol{Q_1} = \boldsymbol{\hat{Q}}^{\mathrm{T}}\boldsymbol{\hat{Q}} \qquad\qquad \boldsymbol{Q_2} = 10^9\boldsymbol{I} \quad (20)$$

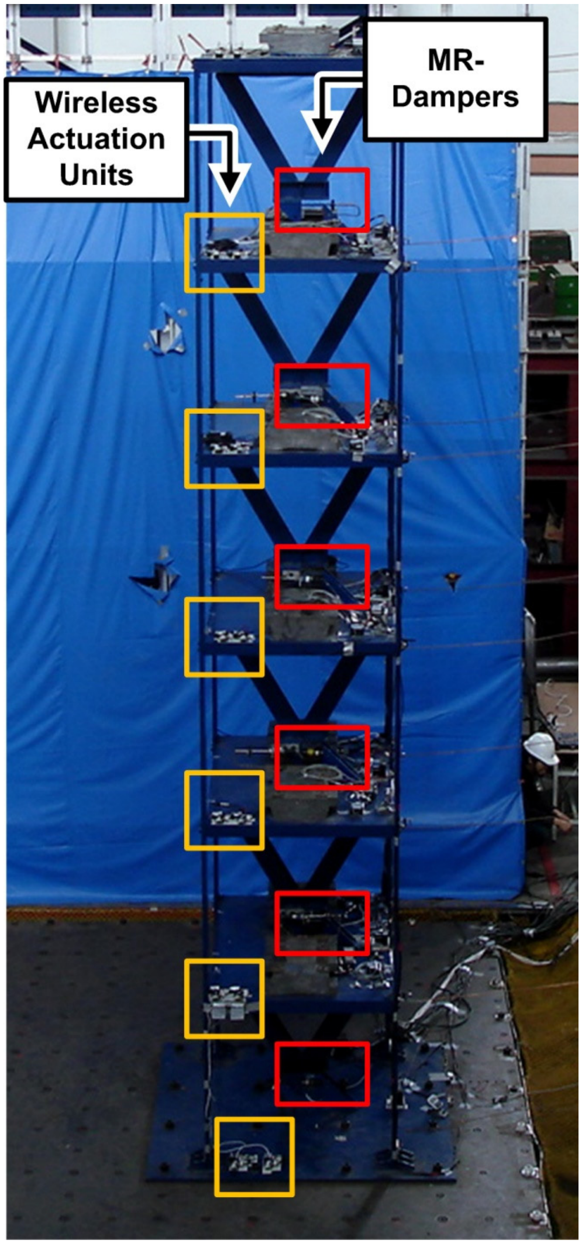

Fig. 2. Six-story laboratory test specimen with wireless sensors and MR-dampers installed.

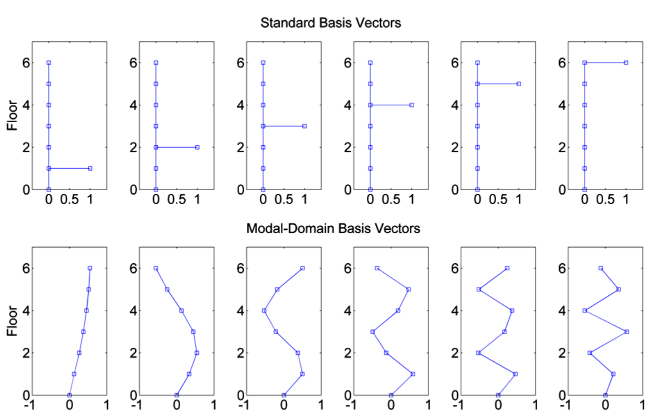

Fig. 3. Standard and modal basis vectors.

$$\widehat{\boldsymbol{Q}} = \begin{bmatrix} \boldsymbol{c\Psi} & \boldsymbol{0} \\ \boldsymbol{0} & \boldsymbol{I\Psi} \end{bmatrix} \quad \boldsymbol{c} = \begin{bmatrix} 9 & 0 & 0 & 0 & 0 & 0 \\ -9 & 4 & 0 & 0 & 0 & 0 \\ 0 & -4 & 1 & 0 & 0 & 0 \\ 0 & 0 & -1 & 1 & 0 & 0 \\ 0 & 0 & 0 & -1 & 1 & 0 \\ 0 & 0 & 0 & 0 & -1 & 1 \end{bmatrix} \tag{21}$$

Control forces are provided by MR-dampers on the structure. The simulation computes the loads applied through use of a bi-linear, bi-viscous, hysteretic damper model [15] with a saturation force of 2.0 kN. Simulated wireless sensor and actuation nodes collect acceleration or drift data from their local floor, transmit it to the network, use this data to update the Kalman estimation of the state vector, compute control forces, and use a look-up table of achievable forces to decide upon a command voltage. Structural response is modeled using Newmark integration (average acceleration method) [14].

The time required to complete a single control step on the *Narada* wireless platform is calculated and incorporated into the simulation. This time step consists of fixed length activities (*e.g.*, sampling, communication, and calculating command voltages) and model-dependent activities (*e.g.*, calculating state estimates and control forces). These values are experimentally derived, and represented in Table 1.

Table 1. Sampling time derivation.

Modes Retained	*Fixed Time (ms)*	*LQR Time (ms)*	*Estimator Time (ms)*	*Total Time (T_s) (ms)*
6	16	1	24	41
5	16	0.7	18.3	35
4	16	0.5	13.5	30
3	16	0.3	9.7	26
2	16	0.2	6.8	23
1	16	0.1	3.9	20

It can be seen that the size of the time step increases in an approximately affine manner, with a slope of about 4 ms/mode over the range of model sizes studied. Structural response using the same excitation record is computed using model sizes ranging from one retained mode to all six modes retained.

C. *Experimental Setup*

The experimental setup is intended to closely mirror the simulation setup. The laboratory structure depicted in Fig. 1 is installed on a 5m x 5m, shaking table (capable of supplying 6-DOF excitations) and excited in the lateral strong direction. Lateral braces are connected to each floor of the structure and support Lord Corp. RD-1005-3 MR-dampers that provide the lateral control forces. *Narada* wireless sensor and actuation units are placed on each floor and connected to transducers. Two series of tests are performed. In the first series, the wireless units are provided acceleration measurements from their associated floor. A seventh unit monitors ground acceleration and broadcasts it

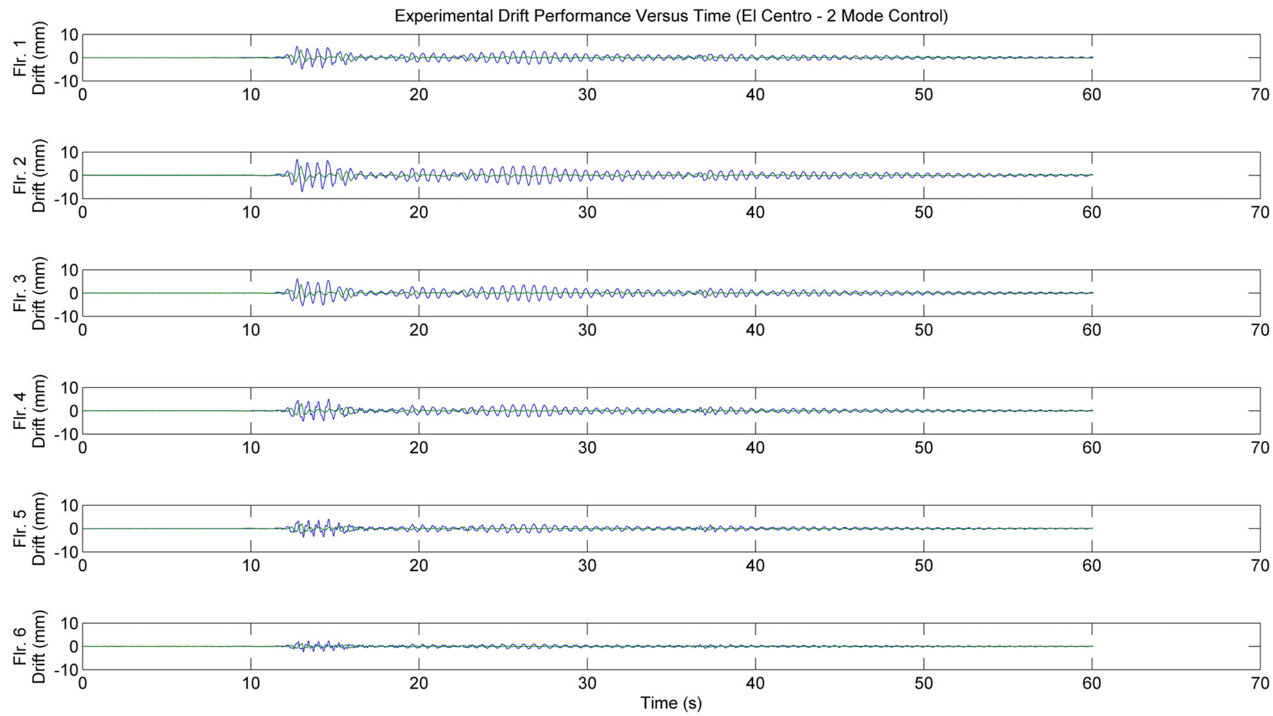

Fig. 4. Controlled and uncontrolled time-history results for inter-story drift.

to the network. In the second series, LVDTs measure inter-story drift at the damper braces. In both setups, *Narada* units calculate their control forces based on models of varying sizes and command collocated MR-dampers. The analog voltage output signals of the *Narada* units are amplified and converted into equivalent current signals before being fed into the damper. After each ground motion record is applied, the wireless network reports its collected data to a PC for off-line analysis. A parallel tethered data acquisition system records structural response, command voltages, and ground motion for validation.

IV. Results

The system was able to mitigate the seismically induced disturbances in terms of minimizing peak drift during excitation with acceleration feedback performing generally better than drift feedback. Results from a representative experimental excitation record (using acceleration feedback and a model based on the first two dynamic modes of the structure) are presented in Fig. 4. The figure shows the inter-story drift for the controlled structure overlaid with the record from the uncontrolled structure (subject to the same excitation) for comparison. To get a more quantitative measure of the effectiveness of the controller, a performance function is proposed for peak drift by which the performance of the controller is normalized by the response of the uncontrolled structure [16]:

$$J = \frac{\max_{Floor,t}(|\,drift_{\mathbf{controlled}}\,|)}{\max_{Floor,t}(|\,drift_{\mathbf{uncontrolled}}\,|)} \tag{22}$$

The performance function is computed for different model sizes to give an indication of the dependency of control performance on model size and time step. The performance function is plotted versus model size for the simulation study (Fig. 5) and experimental study (Fig. 6) under acceleration feedback. In general, there is good agreement between the experimental and simulation results. The performance of the lowest order models suffer due to inaccuracies resulting from the exclusion of the high-frequency modes of the structure. As the model size increases, the controller performance improves up to a model size of four or five modes, and then performance begins to decline. In the experimental portion of the study, a sharp decline in performance is observed for the controller based on the full set of six modes of the structure that is not predicted by the simulation. Later analysis revealed that some unexpectedly high data packet loss occurred during the full six-mode controller test that would account for that discrepancy.

V. Discussion and Conclusions

This study demonstrates that, in resource limited wireless sensor networks, there exists a tradeoff between model size and latency that affects control performance. As model size increases, floating-point computations within the wireless sensor nodes begin to consume more time. Under a constant

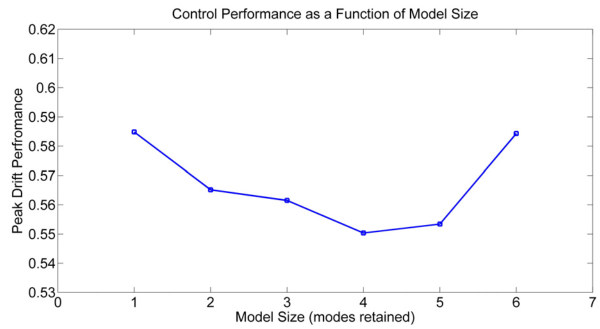

Fig. 5. Simulated control performance of the acceleration feedback controller for six different model sizes.

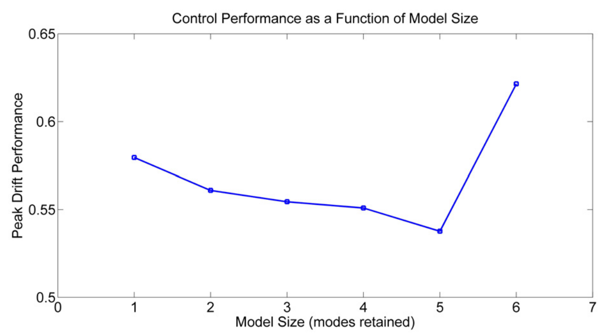

Fig. 6. Experimentally derived control performance of the acceleration feedback controller for six different model sizes.

sample and actuation rate, the increase in model size will result in improved state estimates and improved control performance. When computational demands increase, the sample and actuation rate decrease, degrading the performance. This paper demonstrates that on a six-DOF system that the loss in performance becomes significant compared with the effect of model size. Using a series of reduced-order models derived using model condensation methods; control performance degrades with model size. However, when increased latency due to computations is considered, the performance of controllers based on the larger models is diminished and an optimal model size becomes apparent.

Additional work is warranted in characterizing the optimal model size for arbitrary plants and control objectives. In addition, the control latencies that are presented in this study are hardware specific. Actuator nodes based on newer, faster microcontrollers may soon be available and will alter the balance between model size and latency. It is expected that such actuator nodes will be able to handle larger models with more degrees of freedom before latency begins to be an issue, but validation of the fact and characterization of that tradeoff will be necessary when and if such devices become available. In addition, this study focuses on a very simplistic modal condensation method. More sophisticated approaches have been proposed in the literature (ignored here to limit the number of variables) for control using reduced order systems and should be evaluated in this application to try to reduce the negative effect of the unmeasured modes.

Acknowledgment

The author would like to express his gratitude to Prof. Jerome P. Lynch of the University of Michigan, Ann Arbor, MI, and Prof. C.-H. Loh of National Taiwan University, Taipei, R.O.C. as well as the students and staff of the National Center for Research in Earthquake Engineering (NCREE), Taipei, R.O.C. for invaluable material, moral, and intellectual support.

References

[1] J. T. P. Yao, "Concept of structural control," *Journal of the Structural Division,* vol. 98, pp. 1567-1574, 1972.

[2] B. F. Spencer and S. Nagarajaiah, "State of the art of structural control," *Journal of Structural Engineering,* vol. 129, pp. 845-856, 2003.

[3] G. W. Housner*, et al.*, "Structural control: past, present, and future," *Journal of Engineering Mechanics,* vol. 123, pp. 897-971, 1997.

[4] S. Y. Chu*, et al.*, *Active, Hybrid, and Semi-Active Structural Control: a Design and Implementation Handbook*. New York, NY: Wiley, 2005.

[5] M. Celebi, "Seismic Instrumentation of Buildings (with Emphasis on Federal Buildings)," United States Geologic Survey (USGS), Menlo Park, CA 0-7460-68170, 2002.

[6] Kajima Corporation, "Advanced Structural Control Technologies, HiDAX: High Damping System in the Next Generation," Kajima Corporation, Tokyo, Japan, Corporate Info2006.

[7] Y. Wang*, et al.*, "Wireless feedback structural control with embedded computing," in *Proceedings of SPIE--11th International Symposium on Nondestructive Evaluation for Health Monitoring and Diagnostics*, San Diego, CA, 2006.

[8] Y. Wang*, et al.*, "Decentralized civil structural control using a real-time wireless sensing and control system," in *4th World Conference on Structural Control and Monitoring (4WCSCM)*, San Diego, CA, 2006.

[9] Y. Wang*, et al.*, "Decentralized civil structural control using real-time wireless sensing and embedded computing," *Smart Structures and Systems,* vol. 3, pp. 321-340, 2007.

[10] R. A. Swartz and J. P. Lynch, "Strategic utilization of limited bandwidth in a wireless control system for seismically excited civil structures," *Journal of Structural Engineering,* vol. 135, pp. 597-608, 2009.

[11] R. F. Stengle, *Optimal Control and Estimation*. Mineola, NY: Dover Publications Inc., 1994.

[12] G. F. Franklin*, et al.*, *Feedback Control of Dynamic Systems*, 4th ed. Upper Saddle River, NJ: Prentice Hall, 2002.

[13] R. A. Swartz*, et al.*, "Design of a wireless sensor for scalable distributed in-network computation in a structural health monitoring system," in *5th International Workshop on Structural Health Monitoring*, Stanford, CA, 2005.

[14] A. K. Chopra, *Dynamics of Structures: Theory and Applications to Earthquake Engineering*. Upper Saddle River, NJ: Prentice Hall, 2001.

[15] P.-Y. Lin*, et al.*, "System identification and real application of a smart magneto-rheological damper," in *2005 International Symposium on Intelligent Control*, Limassol, Cyprus, 2005.

[16] Y. Ohtori*, et al.*, "Benchmark control problems for seismically excited nonlinear buildings," *Journal of Engineering Mechanics,* vol. 130, pp. 366-385, 2004.